Available online at www.sciencedirect.com

ScienceDirect

Energy Procedia 137 (2017) 406–413

Energy Procedia

www.elsevier.com/locate/procedia

14th Deep Sea Offshore Wind R&D Conference, EERA DeepWind'2017, 18-20 January 2017, Trondheim, Norway

Control of HVDC systems based on diode rectifier for offshore wind farm applications

Ida Flåten*, Gilbert Bergna-Diaz, Santiago Sanchez, Elisabetta Tedeschi

Department of Electric Power Engineering, Norwegian University of Science and Technology, O.S Bragstads Plass 2E, 7491 Trondheim, Norway

Abstract

The transfer of energy from offshore wind farms using HVDC technology is highly dependant on the converter technology used. The conversion through HVDC has conventionally been done by Line Commutated Converters (LCC) or Voltage Source Converters (VSC), by using thyristor rectifiers or IGBTs, respectively. However, 12-pulse diode rectifier at the offshore converter station can be a promising option due to lower conduction losses, reduced installation costs and converter size, and higher reliability. The main drawback is that the overall control strategy needs to adapt to the uncontrollable diode rectifier. This paper describes the system topology and control solutions proposed with the use of diode rectifier. In addition the paper proposes a shifted voltage and frequency droop control strategy related to the Phase Locked Loop (PLL) to improve the control system as an original contribution. The control strategies are validated in Matlab/Simulink.

Peer-review under responsibility of SINTEF Energi AS.

Keywords: Offshore wind energy; HVDC; Diode rectifier; Control system

1. Introduction

Energy from offshore wind farms can be an important contribution to a more sustainable energy sector. For offshore wind farms located more than 50-100km offshore, HVDC is favoured over HVAC [1]. In this connection the efficiency, reliability and control possibilities of the converted energy depend highly on the HVDC-converter used.

*Ida Flåten. Tel: 93853461
E-mail address: idalfl@stud.ntnu.no

1876-6102
Peer-review under responsibility of SINTEF Energi AS.
10.1016/j.egypro.2017.10.365

The transmission through HVDC has commonly been done through Line Commutated Converters (LCC) with thyristors controlled by a firing angle. However, Voltage Source Converters (VSC) have been used for more recent HVDC projects, with the main advantage being the control possibilities by using Pulse Width Modulation (PWM) [2]. The 2L-VSC is one of the lower costs converter of the VSC technologies, and the performance and reliability can be further improved by the use of the multilevel VSC or the Modular Multilevel Converter (MMC), that can create a more sinusoidal waveform at the output [3].

Diode rectifiers for HVDC connection have higher efficiency, higher reliability and smaller installation costs than LCC with thyristor rectifiers [4]. The technology also compares favorably, regarding the aforementioned aspects, to VSC. However, the lack of control possibilities when using diode rectifier has been an important reason why the technology has not been used for HVDC transmission [5].

The introduction of offshore wind energy into the power market has led to progressive research in HVDC-technology. Offshore converter station based on diode rectifier has been proposed in publications in [6]-[7]. A similar approach is proposed in [8]. Further the use of diode rectifier for the offshore converter station has been proposed in a hybrid configuration with VSC/MMC topologies in [9]. The use of the diode rectifier for this application is, in addition, an emerging topology in the industry, that is under development by Siemens [10][11].

When using diode rectifier for HVDC connection the control approach of the system needs to adapt to the characteristics of the rectifier. Conventionally, when using LCCs or VSCs, the offshore converter of the HVDC system would control the voltage and frequency of the offshore ac grid. However, since the diode rectifier is uncontrolled this task is proposed to be conducted by the front end inverter of the wind turbine. The back end inverter of each wind turbine will then control the voltage in the dc link [6].

A critical issue in the control system proposed in [6] was the Phase Locked Loop (PLL). This is emphasised in [8], and a fixed reference signal of the phase angle was proposed. The main contribution of this paper is to modify the PLL with an integrated phase angle. Moreover, droop control methodology from microgrids will be applied to the system topology to further improve the control system.

2. Proposed topologies

The proposed topology in [6] is replicated and presented as a one-line diagram in figure 1. The HVDC system model consists of a 12-pulse diode rectifier offshore and a 12-pulse thyristor inverter onshore. The wind turbines are Permanent Magnet Synchronous Generators (PMSGs) with a back-to-back converter connection. V_{wi} is the voltage at the terminal of the front-end inverter. T_{wi} is the transformer of each wind turbine, where $i \in \{1, ..., n\}$ with n being the number of turbines. Further, C_F is the filter capacitor at the Point of Common Coupling (PCC), and V_F the voltage at PCC. The ac-side rectifier current is I_{Rac}.

Moreover, the system model proposed in [8] is similar, but with an onshore MMC. In addition the use om both PMSGs and Double Fed Induction Generators (DFIGs) is considered.

3. Operation and control

The development of a control system that allows the control of voltage amplitude and frequency of the offshore ac grid, also in presence of the offshore diode rectifier is presented. The back-end-converter of the wind turbine will control the voltage in the dc-link, while the front end converter will provide the grid integration of the wind turbine controlling the voltage and frequency of the offshore ac-grid. The current, voltage and frequency control in section 3.1 and 3.2 are based on the control method proposed in [6].

3.1. Current control

When applying Kirchhoff's Voltage Law (KVL) to the one-line diagram presented in figure 1, equation (1) is obtained. R and L corresponds to the resistance and inductance of the transformer T_{wi}. I_{Fi} is the front end converter current.

$$[V_{Wi}]^{abc} - [V_F]^{abc} = RI_{Fi}^{abc} + L\frac{dI_{Fi}^{abc}}{dt} \tag{1}$$

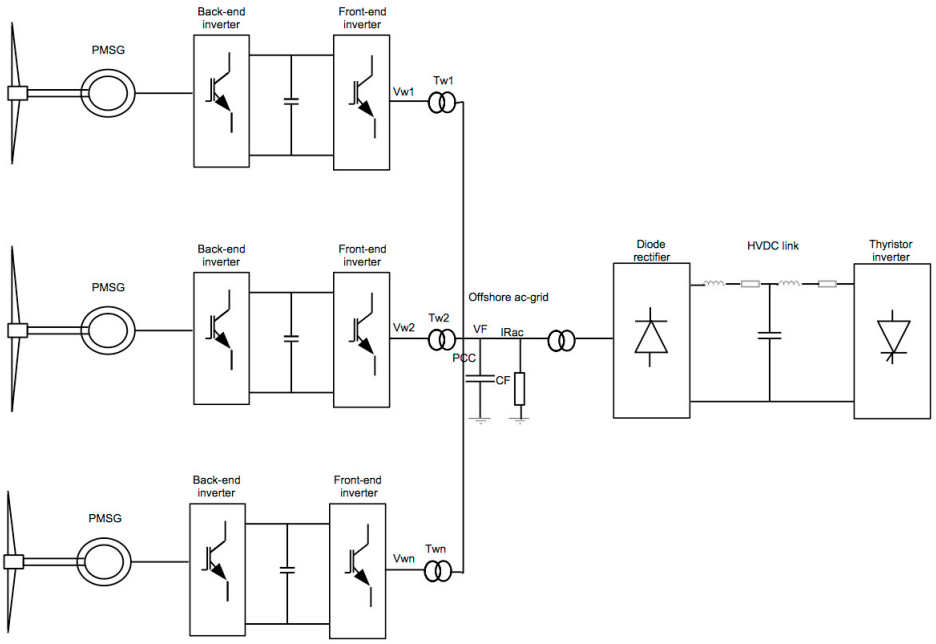

Figure 1: Diode rectifier as offshore HVDC converter - Proposed system topology from [6]

Applying Park transformation and separating the equation into d and q axis in the synchronous reference frame, the previous equation is transformed to equation (2) and (3) where ω is the angular electrical frequency in rad/s, that make up the base for the inner current control loop of the system. This is done by designing PI-controllers local to each front end converter with feed-forward and decoupling terms, with the aim of removing the two last elements of the equations presented. In addition by aligning the d-axis of the selected synchronous reference frame to the V_F vector, the V_F^q component can be assumed to be zero.

$$L\frac{dI^d}{dt} = -RI_{Fi}^d + V_{Wi}^d - V_F^d + L\omega I_{Fi}^q \tag{2}$$

$$L\frac{dI^q}{dt} = -RI_{Fi}^q + V_{Wi}^q - V_F^q - L\omega I_{Fi}^d \tag{3}$$

3.2. Voltage and frequency control

Applying Kirchhoff's Current Law (KCL) to the one-line diagram presented in figure 1, the system equations used to obtain the outer voltage and frequency control loop are obtained. Applying Park transformation and separating into d and q axis the following equations are obtained:

$$C\frac{dV_F^d}{dt} = I_F^d - I_{Rac}^d + C\omega V_F^q \tag{4}$$

$$C\frac{dV_F^q}{dt} = I_F^q - I_{Rac}^q - C\omega V_F^d \tag{5}$$

The voltage and frequency control loops are also based upon the assumption that $V_F^q = 0$, due to the orientation of the synchronous reference frame. Neglecting V_F^q it is seen from equations (4) and (5) that ω is only present in equation (5). Therefore equation (4) is used for the voltage control, while equation (5) is used for the frequency control.

The PI-controller that makes the basis for the voltage control loop is shown in equation (6). Since V_F is a common variable for all the front-end converters, having a PI-controller in each converter would not be

possible. Therefore it is proposed in the literature to have a P-controller local to each converter, and one PI-controller centralized for the whole wind farm.

$$I_F^{d*} = [K_P(V_F^{d*} - V_F^d) + K_I \int (V_F^{d*} - V_F^d)dt] + I_{Rac}^d \tag{6}$$

The frequency control loop is constructed from equation (5). However, since this open loop is sensitive to C_F and a distant measurement of I_{Rac}^q is needed, estimating I_{Rac}^q by using variables local to the wind turbine is proposed in the literature. This is done by using the power equations of each wind turbine. The measurement of I_{Rac}^q is then obtained as follows, where ω_F is the ac-grid frequency:

$$I_{Rac}^q = \frac{1}{3K_{qi}} \frac{V_W^q P_{Wi} - V_W^d Q_{Wi}}{V_W^{d2} + V_W^{q2}} - C_F \omega_F V_F^d \tag{7}$$

The frequency control loop containing the measurement of I_{Rac}^q is presented in figure 2 [6].

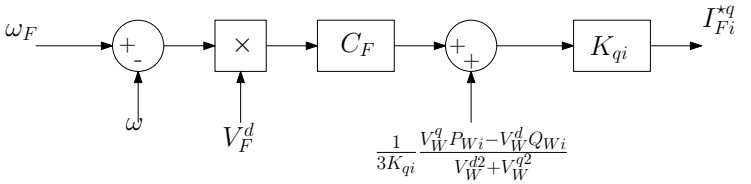

Figure 2: Frequency control loop proposed in [6]

3.3. Phase Locked Loop (PLL)

The PLL extracts the voltage signal at the PCC to determine the phase angle and frequency of the grid, and is an essential part of the control strategy presented.

The power flow of the system with diode rectifier is unidirectional, which implies that a voltage source is not available at the PCC, and thereby the traditional PLL can not serve its function. It is therefore proposed a method called FixRef in [12] which uses an external reference signal of the frequency and phase angle, communicated as GPS time signal or radio signal to avoid the dependence on the voltage signal at the PCC.

Another alternative to the traditional PLL is to modify it appropriately. In [13], a PLL with an integrated phase angle reference is described. This PLL is presented by equation (8) and the deviation from the traditional PLL would be the additional term ω^*.

$$\frac{d\theta}{dt} = \omega^* + \Delta\omega = \omega^* + K_P(V^q - V^{q*}) + K_I \int (V^q - V^{q*})dt \tag{8}$$

This PLL can be viewed as a combination between the traditional PLL and FixRef. Implementing this scheme into the control system proposed by in [6], will be a contribution of this paper to improve the control system performance and avoid synchronization problems.

3.4. Droop control

Instead of using the control approach for frequency and voltage as presented in section 3.1 and 3.2, the concept of voltage and frequency droop control can be applied to the system topology with diode rectifier. The original approach presented in [6] was later changed and developed into a droop control approach for the same system topology in [7]. The droop control approach is not described in detail in [7] and therefore, and for further improvements, contributions from droop control methodology from microgrids [14] will be used in this paper. A detailed explanation of droop control can be found in [15]. In this paper the droop control is named by Output/Input terminology considering the control loop.

3.4.1. P/V and Q/f droop control

The droop control can be constructed from strategies commonly presented for microgrids [14], but considering P/V and Q/f relations, where P is active power and Q is reactive power. These relations can be seen from the system equations (4) and (5), where ω only can be controlled by the q-component of I_F, and thereby the d-component of I_F will control the voltage V_F^d. Controlling I_F^d and I_F^q is proportional to the control of P and Q. It is seen from equation (5) that when ω is reduced I_F^q has to increase to maintain the balance. The line equation presented in (9) is used to describe the droop behaviour.

$$m = \frac{Y_2 - Y_1}{X_2 - X_1} \tag{9}$$

where Y is ω and X is I_F^q for the frequency control. The same slope, m, was then used as follows:

$$I_F^{q*} = I_{Fref}^q - \frac{1}{m}(\omega_{ref} - \omega_m) \tag{10}$$

I_F^{q*} will be the output of the frequency droop control, and then be the input to the current control loop. The voltage control loop can be constructed with the same methodology, by using equation (5). In this case Y is V_F^d, and X is I_F^d. The slope, m, is then used as follows:

$$I_F^{d*} = I_{Fref}^d - \frac{1}{m}(V_{Fref}^d - V_{Fm}^d) \tag{11}$$

3.4.2. P/V and f/Q droop control

In some cases it is preferable that ω is the output of the control system. This case is chosen to be named f/Q, meaning that f is the output while Q is the input. Equation (10) is then solved with respect to ω_{ref}, which can be used as the input to the modified PLL presented in equation (8). When the f/Q strategy is used, I_F^q is not an output of any of the control loops. An additional simple P-control loop with V_F^q as input and I_F^q as output can then be constructed.

4. Simulation and results

The topology in figure 1 with the control strategies presented was made in Matlab/Simulink [16]. The initial aim of the simulation is to examine the use of conventional PLL, FixRef and the modified PLL. An aggregated model of the wind turbines was implemented for this purpose and the control strategies presented in [6] constructed. An essential assumption in the control method proposed is that $V_F^q = 0$ and this is thereby visualised for all three cases.

Secondary, the voltage and frequency droop control strategies were applied to further improve the control system. For this a distributed model consisting of two turbines was carried out. The system parameters used for both the aggregated model and the distributed model are shown in Table 1 in the appendix.

4.1. Aggregated model

4.1.1. Case 1: PLL

The PLL requires a voltage source at the PCC to extract the phase angle and frequency from the voltage signal and therefore the diode rectifier is modeled as a voltage source for this case.

With PLL, V_F^q is assumed to be zero, since the PLL assures no phase shift. When the corresponding Park transformation is used this results in only the first component V_F^d. The voltage V_F is visualised in figure 3(a). Compared to V_F^d, V_F^q can be neglected. Additional simulations, that are not presented due to the space limitations, showed that the current and voltage control loops follow their respective references, while the frequency loop is not capable to follow its imposed reference. This could be due to the voltage source, that enforce the frequency to stay at 50Hz.

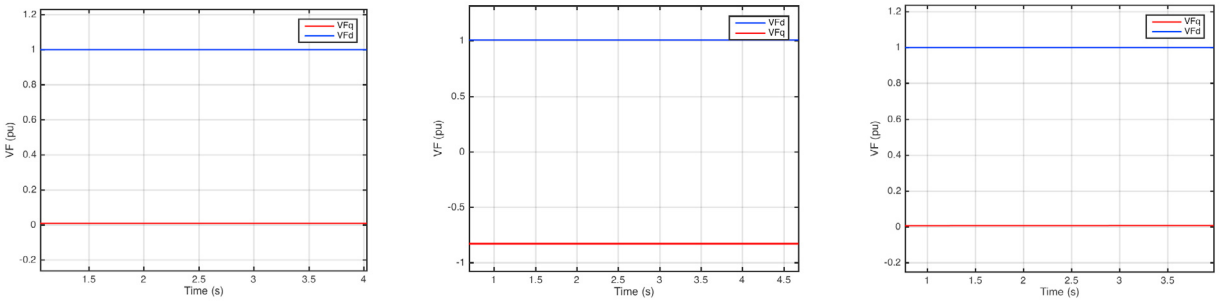

Figure 3: The voltage V_F, at the point of common coupling (PCC) using (a) PLL; (b) FixRef; and (c) modified PLL

4.1.2. Case 2: FixRef

The external phase angle reference, FixRef, is not dependant on a voltage source. The diode rectifier is therefore modeled as a resistance.

The external phase angle does not assure that the phase shift is zero as done by the PLL. When applying Park transformation, V_F^q can thereby not be neglected. This is visualised in figure 3(b).

The simulation results also show that the voltage loop and the current loop are not able to follow their reference when FixRef is applied to the control method presented in [6]. This could be because the assumption $V_F^q = 0$ is no longer valid.

4.1.3. Case 3: Modified PLL

The PLL with integrated phase angle does not require a voltage source and the diode rectifier is modelled as a resistance. When using the modified PLL, the PLL will maintain the characteristics of the conventional PLL and assure no phase shift and thereby V_F^q can be assumed negligible. The current, voltage and frequency loop presented in [6] can therefore be applied. The voltage at the PCC is shown in figure 3(c).

The frequency control loop is visualised in figure 4, where a reference step from 50Hz to 49.5Hz is imposed at t=2s. It is seen that the measured value is following its reference although with a deviation from the imposed reference value. The PLL with integrated phase angle is thereby chosen for further simulations.

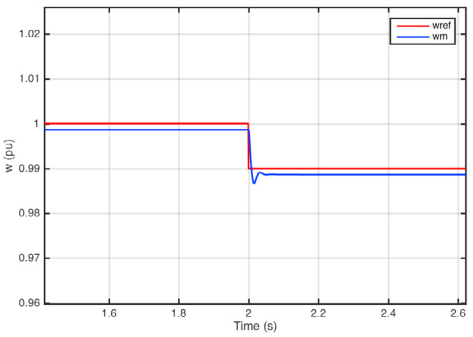

Figure 4: Frequency reference step of 25% at t=2s, using modified PLL Aggregated model

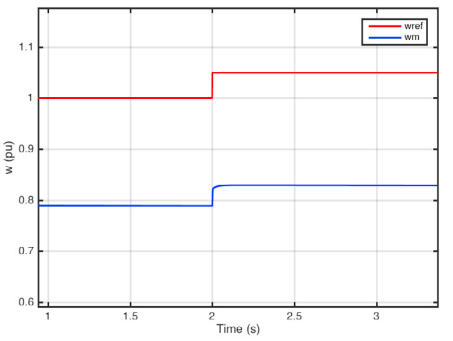

Figure 5: Frequency reference step of 5% at t=2s, using modified PLL Distributed model

4.2. Distributed model

4.2.1. P/V and Q/f droop

The droop control presented was implemented in a two turbine system. With this method the frequency, voltage and current control loop follow their reference, but they all have a significant steady state error. The frequency deviation, with a simulation of a positive step of 5% at t=2s, is shown in figure 5 as an example.

Under the same condition it is found that V_F^q is no longer zero as shown in figure 6(a). This could be because the PI-controller in the current control loop is not working at the frequency it was designed for. Due to this further improvement of the droop control is required, as explained in section 4.2.2.

4.2.2. P/V and f/Q droop

The P/V droop is maintained, while the Q/f curve is shifted, so that f is the output. The frequency will then be used as the integrated phase angle reference in the PLL. With this method the simulation results show that V_F^q is zero, which is seen from figure 6(b).

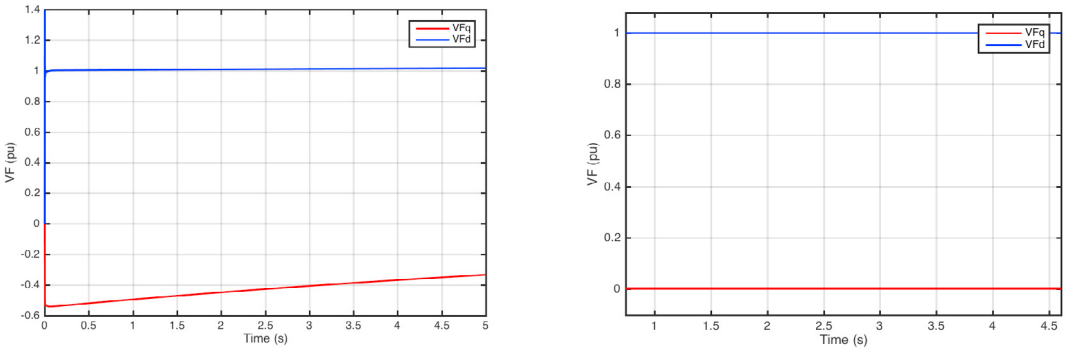

Figure 6: The voltage, V_F, at PCC in with (a) P/V and Q/f droop control and (b) P/V and f/Q droop control

5. Conclusion

Control strategies for frequency and voltage control of the front end converter have been presented as proposed in studied literature. A crucial part of the control strategy was the implementation of the PLL, since the control strategy was based on the assumption that $V_F^q = 0$. However, the conventional PLL could not serve its function without a voltage signal. An attempt was to apply FixRef as proposed in [12][8], a method independent of the voltage signal, but that did not guarantee that $V_F^q = 0$. This issue was solved by the use of PLL with integrated phase angle, which kept the characteristics of the conventional PLL, but was independent of a voltage signal at the PCC.

When the issue of PLL was enhanced, the control strategies was further improved. The control strategy was changed, and droop control methodology was implemented to further improve the control system. The use of the f/Q droop technique allowed reactive power sharing between the wind turbines. However, the active power control was made in a master-slave technique, where only one turbine was controlling the power. Droop application for active power control is the subject of further work.

Appendix A

Table 1: System parameters

Wind turbine		
Power	100	MW
Voltage	0.69	kV
Leakage reactance	0.1	pu
Resistance	0.011	pu
Switching frequency	2	kHz
Offshore ac grid		
Voltage	0.69	kV
Frequency	50	Hz
Capacitor Bank	100	MVA
HVDC Rectifier		
Leakage reactance	0.18	pu
Resistance	0.1	pu
HVDC	400	kV

References

[1] G. F. Reed, H. A. A. Hassan, M. J. Korytowski, P. T. Lewis, B. M. Grainger, Comparison of hvac and hvdc solutions for offshore wind farms with a procedure for system economic evaluation, in: Energytech, 2013 IEEE, 2013, pp. 1–7. doi:10.1109/EnergyTech.2013.6645302.

[2] R. Adapa, High-wire act: Hvdc technology: The state of the art, in: IEEE Power and Energy Magazine, Vol. 10, 2012, pp. 18–29. doi:10.1109/MPE.2012.2213011.

[3] U. N. Gnanarathna, A. M. Gole, R. P. Jayasinghe, Efficient modeling of modular multilevel hvdc converters (mmc) on electromagnetic transient simulation programs, IEEE Transactions on Power Delivery 26 (1) (2011) 316–324. doi:10.1109/TPWRD.2010.2060737.

[4] J. P. Bowles, Multiterminal hvdc transmission systems incorporating diode rectifier stations, IEEE Transactions on Power Apparatus and Systems PAS-100 (4) (1981) 1674–1678. doi:10.1109/TPAS.1981.316562.

[5] S. Bernal-Perez, S. Ano-Villalba, R. Blasco-Gimenez, J. Rodriguez-D'Derlee, Efficiency and fault ride-through performance of a diode-rectifier- and vsc-inverter-based hvdc link for offshore wind farms, IEEE Transactions on Industrial Electronics 60 (6) (2013) 2401–2409. doi:10.1109/TIE.2012.2222855.

[6] R. Blasco-Gimenez, S. A-Villalba, J. Rodrguez-DDerle, F. Morant, S. Bernal, Distributed voltage and frequency control of off-shore wind farms connected with a diode based hvdc link, in: IECON 2010 - 36th Annual Conference on IEEE Industrial Electronics Society, 2010, pp. 2994–2999. doi:10.1109/IECON.2010.5674956.

[7] A. I. Andrade, R. Blasco-Gimenez, G. R. Pena, Distributed control strategy for a wind generation systems based on pmsg with uncontrolled rectifier hvdc connection, in: 2015 IEEE International Conference on Industrial Technology (ICIT), 2015, pp. 982–986. doi:10.1109/ICIT.2015.7125225.

[8] C. Prignitz, H. G. Eckel, S. Achenbach, F. Augsburger, A. Schn, Fixref: A control strategy for offshore wind farms with different wind turbine types and diode rectifier hvdc transmission, in: 2016 IEEE 7th International Symposium on Power Electronics for Distributed Generation Systems (PEDG), 2016, pp. 1–7. doi:10.1109/PEDG.2016.7527013.

[9] T. H. Nguyen, Q. A. Le, D. C. Lee, A novel hvdc-link based on hybrid voltage-source converters, in: 2015 IEEE Energy Conversion Congress and Exposition (ECCE), 2015, pp. 3338–3343. doi:10.1109/ECCE.2015.7310131.

[10] P. Menkel, New grid access solutions for offshore wind farms.
URL `http://www.ewea.org/offshore2015/conference/allposters/PO208.pdf`

[11] Siemens, New dc grid access solution.
URL `http://www.energy.siemens.com/nl/pool/hq/power-transmission/grid-access-solutions/dc-solutions/DC-Flyer.pdf`

[12] M. Gierschner, H. J. Knaak, H. G. Eckel, Fixed-reference-frame-control: A novel robust control concept for grid side inverters in hvdc connected weak offshore grids, in: Power Electronics and Applications (EPE'14-ECCE Europe), 2014 16th European Conference on, 2014, pp. 1–7. doi:10.1109/EPE.2014.6910711.

[13] S. Sanchez, Stability Investigation of Power Electronic Systems A Microgrid Case, Doctoral thesis at NTNU (2015:2).
URL `https://brage.bibsys.no/xmlui/handle/11250/281238`

[14] J. M. Guerrero, J. C. Vsquez, R. Teodorescu, Hierarchical control of droop-controlled dc and ac microgrids x2014; a general approach towards standardization, in: Industrial Electronics, 2009. IECON '09. 35th Annual Conference of IEEE, 2009, pp. 4305–4310. doi:10.1109/IECON.2009.5414926.

[15] K. D. Brabandere, B. Bolsens, J. V. den Keybus, A. Woyte, J. Driesen, R. Belmans, A voltage and frequency droop control method for parallel inverters, IEEE Transactions on Power Electronics 22 (4) (2007) 1107–1115. doi:10.1109/TPEL.2007.900456.

[16] I. Flåten, Control of hvdc systems based on diode rectifier for offshore wind farm applications, Project thesis at NTNU 2016.